
MotifDisco: Motif Causal Discovery For Time Series Motifs

Josephine Lamp, Mark Derdzinski, Christopher Hannemann,
Sam Hatfield, Joost van der Linden
Dexcom, USA*

Abstract

Many time series, particularly health data streams, can be best understood as a sequence of phenomenon or events, which we call *motifs*. A time series motif is a short trace segment which may implicitly capture an underlying phenomenon within the time series. Specifically, we focus on glucose traces collected from continuous glucose monitors (CGMs), which inherently contain motifs representing underlying human behaviors such as eating and exercise. The ability to identify and quantify *causal* relationships amongst motifs can provide a mechanism to better understand and represent these patterns, useful for improving deep learning and generative models and for advanced technology development (e.g., personalized coaching and artificial insulin delivery systems). However, no previous work has developed causal discovery methods for time series motifs. Therefore, in this paper we develop *MotifDisco* (**motif discovery of causality**), a novel causal discovery framework to learn causal relations amongst motifs from time series traces. We formalize a notion of *Motif Causality (MC)*, inspired from Granger Causality and Transfer Entropy, and develop a Graph Neural Network-based framework that learns causality between motifs by solving an unsupervised link prediction problem. We integrate MC with three model use cases of forecasting, anomaly detection and clustering, to showcase the use of MC as a building block for downstream tasks. Finally, we evaluate our framework on different health data streams and find that Motif Causality provides a significant performance improvement in all use cases.

1 Introduction

Many time series can be best understood as sequences of phenomenon or events. This is extremely common in many health data streams where traces are guided by underlying human physiology or behaviors. We call these events in the traces *motifs*. A time series motif is a short trace segment which may implicitly capture an underlying behavior or phenomenon within the time series. To contextualize our discussion, and as our main running example, we focus on glucose traces collected from continuous glucose monitors (CGMs) for diabetes. Glucose traces inherently contain motifs which represent underlying human behaviors. For instance, a motif capturing a peak in glucose may correspond to an individual eating; a motif capturing a drop in glucose may correspond to an individual exercising. Figure 1 shows real glucose traces and motifs (other examples in Appx. A.1).

Causal discovery is the process by which causal relations are found amongst observational data [1]. The ability to discover and quantify causality amongst motifs can provide a mechanism to better understand and represent these patterns, useful in a variety of applications. For instance, learning causal relations in glucose motifs may enable better understanding of physiological patterns contributing to advanced technology development (e.g., artificial insulin delivery systems). Moreover,

*Disclaimer: The views and opinions expressed in this paper are those of the authors and do not necessarily reflect the official policy or position of Dexcom Inc.

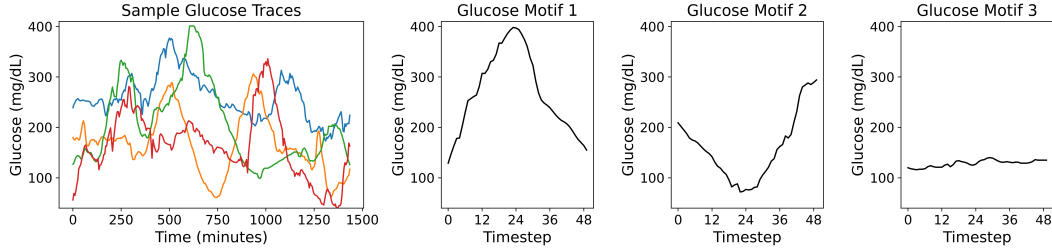


Figure 1: Real Glucose Traces and Sample Motifs for $\tau = 48$.

motif causal relationships may be helpful building blocks when used as sub-components in generative and deep learning models to improve their performance for other downstream tasks.

Granger Causality [2] and its nonlinear extension Transfer Entropy (TE) [3] are commonly used in time series causal discovery methods, as causal relations are quantified based on one trace’s *predictability* of another. This notion of causality provides an intuitive, understandable measure to quantify causal relations and is advantageous for time series because it innately incorporates temporality without requiring strong model assumptions. Despite exciting recent developments for time series causal discovery [4, 5], no previous work has focused on causal discovery amongst time series *motifs*. Motif causal discovery is challenging because in many cases (particularly in health) there is no ground truth about what underlying behavior a motif captures. For example, from data alone one cannot conclusively determine what caused a change in glucose (e.g., a glucose rise may be from eating *or* stress). As a result, unlike in many other causal models, there is no ground truth causal structure amongst motifs that could be used to guide the casual discovery model (i.e., through supervised methods using labeled causal events.)

Therefore, in this paper we develop *MotifDisco*, (**motif discovery** of causality), a framework to discover causal relations from time series motifs. First, we formalize the concept of motifs and define a notion of *Motif Causality* (MC) inspired from Granger Causality and Transfer Entropy, which is able to characterize causal relationships amongst sequences of motifs. Next, we develop a causal discovery framework to learn MC amongst a set of ordered motifs pulled from time series traces. The framework uses a Graph Neural Network (GNN) based architecture that learns causality amongst motifs by solving an unsupervised link prediction problem, thereby not requiring knowledge of any ground truth causal structure for training. The framework outputs a directed causal graph where nodes represent motifs and edges represent the degree of the MC relationship. To demonstrate the suitability of Motif Causality as a building block in other models for downstream tasks, we instantiate three model use cases that incorporate MC for forecasting, anomaly detection, and clustering tasks. Finally, we evaluate *MotifDisco* in terms of scalability and use case performance by comparing the models with and without integration of MC, to see how helpful MC is for each use case.

The contributions of this paper are: (1) We formalize a new notion of causality between time series motifs, denoted as Motif Causality. (2) We develop *MotifDisco*, the first causal discovery framework to learn Motif Causality amongst time series motifs. (3) We illustrate the use of MC as a building block in other downstream tasks by integrating MC with three model use cases of forecasting, anomaly detection and clustering. (4) We provide detailed framework evaluation and find that MC provides a significant performance improvement compared to the base models in all use cases.

2 Related Work

Motifs. Recently, there has been interest in temporal *network motifs*, which are sets of recurring graph substructures. Previous work has investigated network motif causality [6, 7] and developed network motif causal discovery frameworks [8, 9, 10]. Importantly, the definition of motif used here is different than ours, referring to patterns in graph structures as opposed to patterns in the traces themselves. In other motif application areas, Chinpattanakarn and Amornbunchornvej [11] solve a different problem and develop a method to infer a set of patterns, also called motifs, that follow each other in the traces. Finally, Lamp et al. [12] develop a method to generate synthetic time series glucose traces and use a notion of causality amongst motifs to help the model perform well. The

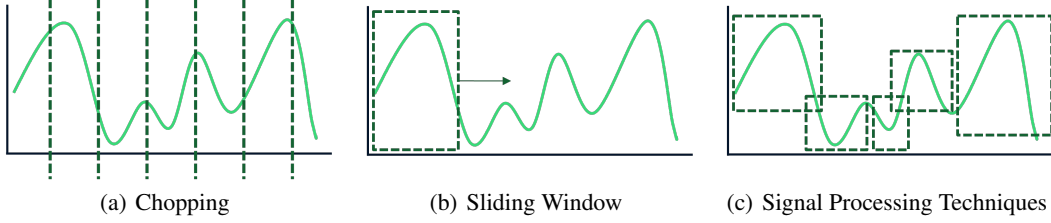


Figure 2: Example Motif Construction Methods: (a) chopping the trace into chunks, (b) using a sliding window, or (c) using signal processing techniques to automatically identify motifs.

focus of this work is not on causality, and the causal learning method is complicated and suffers from scalability issues.

Causal Discovery in Time Series. There are a variety of works on causal discovery for time series [1, 4, 13, 5, 14]. In particular, previous methods have developed causal discovery frameworks for multivariate time series that incorporate temporal dynamics and use Granger Causality [15, 16, 17] or Transfer Entropy [18, 19]. Recent work has also incorporated time series causality measures to improve model learning in downstream tasks such as forecasting and anomaly detection [20, 21, 22, 23, 24]. Previous methods for time series causal discovery cannot be directly applied to motifs because they formulate causality using multivariate statistical properties (e.g., variable-based correlation) or temporal statistical measures repeated across time series lags, which do not hold for short, univariate time series motifs that do not contain repeated lagged patterns; or use labels or known underlying causal structures, which are not available for our traces and many similar event-based data streams. *MotifDisco* is the first framework for causal discovery in time series motifs, which may broaden current model capabilities for event-based time series.

3 Formalizing Motif Causality

Motifs & Motif Construction. We first formalize our notion of motifs. A motif is a short segment of the trace which may implicitly capture an underlying behavior within a time series. Real sample traces and motifs are shown in Figure 1 and Appx. A.1. We define a *motif*, μ , as a short, ordered sequence of values (v) of length τ :

$$\mu = [v_i, v_{i+1}, \dots, v_{i+\tau}] \quad (1)$$

We denote a set of n time series traces as $X = [x^1, \dots, x^n]$. Each time series may be represented as a sequence of motifs: $x^j = [\mu_1^j, \mu_2^j, \dots]$ where each μ_t^j gives the motif identifier i at the ordered time step t . We also define a motif set \mathcal{M} , of $|m|$, which is the complete set of motifs generated from the traces $\mathcal{M} = \{\mu^1, \dots, \mu^m\}$. We assume there is a consistent, conclusive way to pull motifs from the traces; the user may choose which method they use based on the end application goal. Motif discovery is outside the scope of this work since this problem has been widely solved (see [11, 25, 26] and Appx A.2). That being said, three straightforward methods to extract motifs from traces, shown in Figure 2, include chopping the traces into size τ chunks (a), using a sliding window of size τ to extract motifs (b), and using signal processing techniques such as Discrete Fourier Transforms (DFT) to automatically extract motifs (c). Our framework is amenable to any motif extraction method.

Granger Causality & Transfer Entropy. Granger Causality is a common method to characterize causal relations amongst time series [2]. Different from other causal methods, Granger defines causal relations in terms of *predictability*. Under Granger Causality, given two time series x and y , x causes y if past information about x is more predictive than past information about y only. Transfer Entropy (TE), sometimes also called Causation Entropy, is a nonlinear extension of Granger Causality [3, 27]. Using information theoretic measures, TE measures the amount of uncertainty that is reduced in future states of time series y as a result of knowing the past states of time series x . Given two time series, x^i and y^i , the TE from x^i to y^i is:

$$TE_{x^i \rightarrow y^i} = H(y_t^i | y_{t-1, \dots, t-f}^i) - H(y_t^i | y_{t-1, \dots, t-f}^i, x_{t-1, \dots, t-g}^i) \quad (2)$$

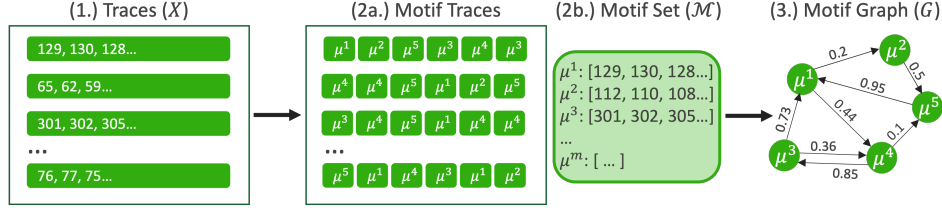


Figure 3: Preprocessing Steps. X are transformed to motif traces and \mathcal{M} and then into a graph G .

where $H(\cdot|\cdot)$ is a conditional entropy function and f and g are lag constants.

Traditional TE is under the important assumption that the effect is influenced by the cause under a fixed, constant time delay. However, this assumption does not hold for many real world time series applications, particularly in health streams, where data may be affected by past events at *varying* lengths of time. As such, an extension of TE that allows for different time delays has been developed, denoted here as Variable-lag Transfer Entropy (VTE) [28]. The VTE from x^i to y^i is defined as:

$$VTE_{x^i \rightarrow y^i} = H(y_t^i | y_{t-1, \dots, t-f}^i) - H(y_t^i | y_{t-1, \dots, t-f}^i, x_{t-1-\Delta_{t-1}, \dots, t-g-\Delta_{t-g}}^i) \quad (3)$$

where Δ_t is a variable length lag amount. We will adapt this equation and other notions of TE next for our definition of Motif Causality.

Defining Motif Causality. Our definition of motif causality is inspired from various Transfer Entropy and Causation Entropy threads (Equation 3, Irribarra et al. [29], Gong et al. [4], Amornbunchornvej et al. [28], Assaad et al. [30], Sun et al. [31]). The Motif Causality (MC) from motif μ^i to motif μ^j conditioned on the set of motifs \mathcal{K} is defined as:

$$MC_{\mu^i \rightarrow \mu^j | \mathcal{K}} = H(\mu_t^j | \mathcal{K}_{t-1, \dots, t-f}) - H(\mu_t^j | \mathcal{K}_{t-1, \dots, t-f}, \mu_{t-1-\Delta_{t-1}, \dots, t-g-\Delta_{t-g}}^i) \quad (4)$$

where $\mathcal{K} \subset \mathcal{M}$, $H(\cdot|\cdot)$ is a conditional entropy function, f and g are lag constants and Δ_t is a variable length lag amount. Essentially, this provides a measure of information gain by determining how much uncertainty is reduced for μ^j by observing past occurrences of μ^i compared to the “status quo”, the set of the rest of the motifs \mathcal{K} . The MC value will be between 0.0 and 1.0. Higher values indicate stronger causality (i.e., more uncertainty about the future is reduced for μ^j given μ^i).

Conditional Entropy Function. To implement the conditional entropy function, $H(\cdot|\cdot)$, there are many different types of entropy which the user can choose based on their end goal or application. For our purposes, we elucidate two common ones: Shannon entropy [32] and Rényi entropy [33, 34]. Shannon entropy is defined as:

$$H(x^i) = - \sum_t p(x_t^i) \log_2(p(x_t^i)) \quad (5)$$

where p is a probability distribution. Rényi is more flexible at estimating uncertainty and defined as:

$$H_\alpha(x^i) = \frac{1}{1-\alpha} \log \left(\sum_{v=1}^n p_v^\alpha(x^i) \right) \quad (6)$$

where α is a weight parameter, $\alpha > 0$. When $\alpha \rightarrow 1$ Rényi entropy converges to Shannon entropy. We note that there are many other types of entropy functions that could be used and might be relevant, such as Wavelet [35] or Permutation Entropy [36].

4 Motif Causal Discovery Framework

Now that we have formulated our definition of Motif Causality, we next describe our casual discovery framework *MotifDisco* to learn motif causal relationships amongst a set of time series motifs. We first detail preliminaries related to the problem definition and preprocessing in Section 4.1, describe the model architecture in Section 4.2 and finish with the model training algorithm in Section 4.3.

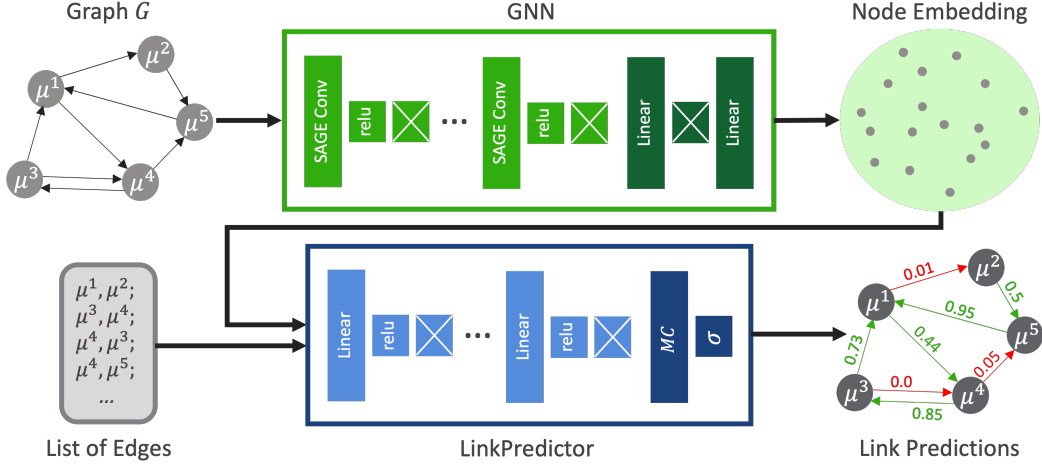


Figure 4: Model Architecture: a GNN consisting of stacks of GraphSAGE, ReLU, Dropout (“X” boxes) and Linear layers learns a node embedding. The LinkPredictor consists of Linear, ReLU and Dropout layers followed by the “MC” motif causality layer and a Sigmoid layer (σ box). The LinkPredictor takes in the node embedding and outputs the predicted edges and their weights.

4.1 Preliminaries

Problem Definition. Since we do not know nor have any way to determine the underlying motif-causal structure (i.e., we have no ground truth), we formulate this problem as an unsupervised graph link prediction problem: Given a set of input time series motifs extracted from our set of traces X , and the complete set of nodes which is equivalent to the motif set \mathcal{M} (i.e., each motif is a node), predict the edges between all the nodes. In other words, learn the edge weights, the motif causal relationships, between all the nodes, the motifs. To solve this problem, we build a Graph Neural Network-based causal discovery framework that learns the MC edge weights in an unsupervised manner. We walk through each part of the framework next, starting with the preprocessing steps.

Preprocessing. An overview is shown in Figure 3. Motifs of length τ are pulled from the input time series to create a set of ordered motif traces and the motif set \mathcal{M} (see Section 3). In our implementation, we use the chopping method to generate motifs; \mathcal{M} is the union of all size- τ chunks in the traces. From there, an initial motif graph is generated from the motif traces. In the graph structure, each node contains the motif identifier and the actual motif values (e.g., motif $\mu^1 = [129, 130, 128, \dots]$). Edges represent directed motif-causal relationships between two motifs. The edge weight indicates the *strength* of the causal relationship. At this stage, generating the *best* graph is not our primary concern since the framework will add and remove optimal edges during the learning process, and we just need a starting graph structure to build from. As such, we believe it an acceptable first pass to assume there is *some* degree of causality between motifs that appear immediately one after the other, and build the preliminary graph by adding edges between each subsequent motif in the traces. For example, for the first motif trace in Fig. 3 (2a), edges would be added from $\mu^1 \rightarrow \mu^2$, $\mu^2 \rightarrow \mu^5$, etc. We compute the MC edge weight according to Equation 4.

4.2 Model Architecture

An overview of the model architecture is shown in Figure 4. The model consists of two main components: a Graph Neural Network (GNN) that uses GraphSAGE layers to learn node embeddings, and a LinkPredictor network that uses the learned node embeddings to predict motif causal links amongst nodes. We detail each component next and then describe model training in Section 4.2.

GNN. The Graph Neural Network takes in a starting motif graph G , and outputs a learned node embedding. The GNN is structured using GraphSage convolutional layers. GraphSAGE (standing for Sample and Aggregate) [37] learns low dimensional vector representations of nodes. The core

Algorithm 1: Training Procedure to Learn Motif Causality

Input: Input Graph G , Epochs e , Edge Prediction Threshold θ

```
1 for  $e$  epochs do
  /* Compute Node Embedding */
2  node_emb = GNN ( $G$ )
  /* Get predictions on positive edges */
3   $E \leftarrow \text{sample}(G.\text{edges})$  // Edges that exist in  $G$ 
4   $p, c = \text{LinkPredictor}(\text{node\_emb}, E)$ 
  /* Get predictions on negative edges */
5   $\hat{E} \leftarrow \text{negative\_sample\_edges}(G)$  // Edges not in  $G$ 
6   $\hat{p}, \hat{c} = \text{LinkPredictor}(\text{node\_emb}, \hat{E})$ 
  /* Compute Loss */
7   $y = \gamma \times p + \lambda \times c$ 
8   $\hat{y} = 1 - (\gamma \times \hat{p} + \lambda \times \hat{c})$ 
9   $\text{loss} = -\sum_{i=1}^b (y_i \log \hat{y}_i + (1 - y_i) \log(1 - \hat{y}_i))$ 
  /* Update edges in the graph based on new predictions */
10  $G.\text{update\_edges}(E, y, \hat{E}, \hat{y}, \theta)$ 
11 end
```

intuition of GraphSAGE is that a node is known by the company it keeps (i.e., its neighbors). The algorithm works by iterating over a sample of the node’s neighboring nodes and “aggregating” their embeddings in order to determine the current node’s embedding. Importantly, GraphSAGE is *inductive*, meaning it can generalize to unseen nodes. GraphSage use both node features and topological structure (i.e., the graph structure) of each node’s neighbourhood simultaneously to efficiently generate representations for new nodes without requiring model retraining. To do this, the algorithm relies on its aggregation function, also known as the message-passing process, which learns how to aggregate node features based on encoding information about a node’s local neighborhood. Therefore, when given new node data, the function uses the local neighborhood of the node to aggregate the features appropriately, and learn the embedded feature representation (as opposed to needing to learn a unique embedding for every individual node). As shown in Figure 4, in our framework the GNN consists of sequential stacks of GraphSAGE convolutional, ReLU and dropout layers (represented by the “X” boxes in the figure) followed by the message-passing layers— stacks of linear and dropout layers. The motif time series values are the node data used to learn the embeddings. We instantiate the aggregation function using mean aggregation for simplicity.

Link Predictor. The LinkPredictor network takes in learned node embeddings outputted from the GNN and a list of edges to predict, and returns the probability of each edge and the motif causality values for each edge. At its core, the LinkPredictor learns a function to predict the probability of an edge between two nodes. To do this, it computes the MC between the nodes using Equation 4, and a probability score, represented by the element-wise dot product of the two embedded node vectors. To implement the MC computation, we adapt existing Transfer Entropy libraries and compute the conditional entropy function, $H(\mu)$, using the histogram method [38]; additional details in Appx. A.2. In terms of architecture, the LinkPredictor is implemented via stacks of linear, ReLU and dropout layers followed by Motif Causality (MC) and sigmoid layers to learn the edge probability function. The network balances evaluating the product of the embedded node vectors and the motif causal values between the motifs themselves, allowing the network to learn how to optimize edge addition/deletion in the graph guided by the underlying causality. (More details provided next in Section 4.3). In this way, the LinkPredictor learns to predict edges that have high motif causality with high probability.

4.3 Model Training

We next describe how the entire framework is trained together, shown in Algorithm 1. First, the graph is fed through the GNN network to learn an embedded representation of the nodes (Line 2). Next, the LinkPredictor makes predictions on a sample of the edges that exist in the graph G , denoted as the positive edges E using the learned node embedding (Line 3-4). Then, a batch of edges that do

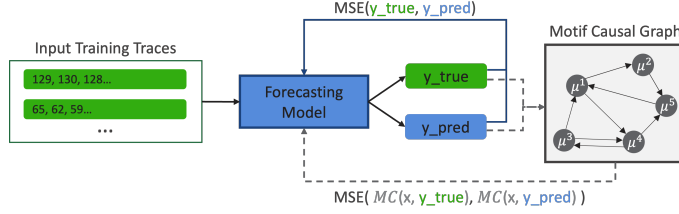


Figure 5: Forecasting Model integrated with Motif Causality.

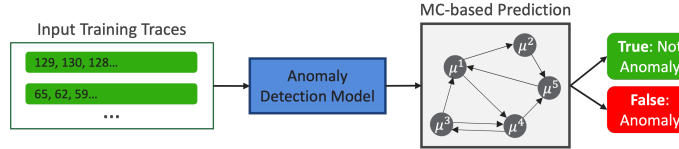


Figure 6: Anomaly Detection Model integrated with Motif Causality.

not exist in G , \hat{E} , are randomly sampled by selecting random pairs of nodes with no connections between them (Line 5). The LinkPredictor makes predictions on the negative edges (Line 6).

From there, the positive predictions y are computed by combining the positive edge predictions p and the motif causality values for the positive links c (Line 7). Similarly, the negative predictions \hat{y} are computed by combining the negative link predictions \hat{p} with the MC values for the negative links \hat{c} (Line 8). γ and λ are important hyper-parameters which balance the influence of the dot product predictions vs. the motif causality. The model is trained to minimize the log likelihood loss function, computed following the equation on Line 9. Essentially, this loss function optimizes the model to maximize its predictions of positive edges (true links, edges that have high motif causality values) and minimize predictions of negative edges (links that should not exist in G , edges with low MC). Finally, the edges in G are updated based on the model edge predictions and an edge threshold θ (Line 10). θ is a user-specified parameter with a range between 0 and 1. If any of the edges in $\hat{y} \geq \theta$, they are added to the graph G ; if any of the edges in $y < \theta$, they are removed from G .

Due to the dual training between the GNN and the LinkPredictor, as the model iterates the node embeddings are continuously updated based on new linkages that may be added or removed. As such, the GNN learns good node embeddings representative of the types of nodes that are close to each other and have connections to each other (nodes that are very motif causal of one another). The LinkPredictor is guided by the motif causality values between motifs to help it predict where linkages should be, and as it learns characteristics of highly causal edges, and gets better and better node embeddings from the GNN, it learns a good prediction function for predicting node linkages.

Making New Edge Predictions. To make a link prediction between two new nodes using the trained framework, the nodes are first fed through the GNN to get their node embeddings, and then the embeddings are sent through the trained LinkPredictor network, which returns the predicted probability they have an edge between them, along with the motif causality value.

5 Uses of Learned Motif Causality

To illustrate the use of Motif Causality as a building block for other downstream tasks, in this section we integrate Motif Causality with three example model use cases of Forecasting, Anomaly Detection and Clustering. We evaluate the performance of these use cases later in Section 6.

Forecasting. Our integration is shown in Figure 5. Briefly, some basic forecasting models work by sliding a window across input traces to learn sequential time series patterns. Their loss function computes the difference between the model’s predicted future timesteps (y_pred) and the ground truth future time steps (y_true) in the traces. To integrate motif causality, we add an additional loss function that seeks to minimize the difference in the MC between the previous time step (x) and the predicted future time steps (y_pred) vs. x and the ground truth future time steps (y_true). The intuition is that

there should be similar causality between the previous time step and the predicted future time step as the ground truth data. MC is computed using the trained motif causal graph outputted from the MC framework. We assume the motif size τ is the same as the forecasted prediction window size to ensure MC is computed on comparable time chunks (i.e., motifs).

Anomaly Detection. Integration of a basic anomaly detection model with MC is shown in Figure 6. We add an MC-based anomaly prediction block after the model that uses the predicted MC between previous timesteps and future timesteps to determine if the next trace chunk may be anomalous or not. Specifically, it checks if the MC between the previous time steps (previous motif) and the next one are less than a threshold, and if so classifies it as an anomaly. The size of the predicted time chunk must be the same size as the motif size τ and we suggest the anomaly threshold be set to the edge prediction threshold θ , since this was what was used to train the motif causal graph originally.

Clustering. For clustering, there is typically a method to group clusters based on minimizing distances between each data point and the cluster centroid. These distances are computed using various distance measures such as Discrete Time Warping (DTW) [39] for traces. To integrate MC with a basic clustering algorithm, we use the motif causality values as an additional distance metric. The intuition here is to add an element of *causality* to the clustering, such that as the algorithm learns, MC values within each cluster will be minimized and similar data points within the cluster should be *motif causal* of each other. An example is shown in Figure 12 in Appx. A.2.

6 Evaluation

As mentioned in Section 2, existing Granger causal techniques are not directly comparable with *MotifDisco* due to their framework set-up or model assumptions; i.e., they formulate causality using multivariate statistical properties or temporal statistical measures using time lags which do not hold for motifs, or require labels or a known underlying causal structure which are not available for our health data streams (see Appx. A.3.) Therefore, in this section we evaluate our causal discovery framework in terms of scalability and performance for three downstream use cases: forecasting, anomaly detection and clustering.

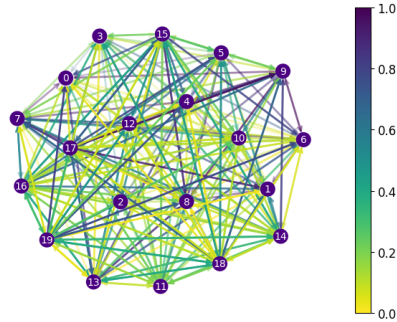


Figure 7: Learned Motif Causal Graph for $n = 10$, $|\mathcal{M}| = 20$. Edge color indicates the MC value.

Experimental Details. We use three health stream datasets with different lengths and sampling frequencies: glucose traces from continuous glucose monitors [40], ECG traces and respiration (Resp) traces from the MIMIC-BP dataset [41]. All experiments were run 5 times with an 80/20% train/test split on an Intel Sky Lake 48 CPU VM with 192GB of RAM. Motifs were pulled from traces using the chopping method and we set $\gamma = 0.7$ and $\lambda = 0.5$. Additional details are available in Appx. A.3.

Motif Causal Graphs. An example motif causal graph from the *MotifDisco* framework is shown in Figure 7. The edge color indicates the strength of the MC relationship; darker is stronger (closer to 1) while lighter is less strong (closer to 0). A.3.4 shows example MC between motifs of different τ .

Scalability. Scalability evaluation is shown in Figure 8 and Appx. A.3.2, computing total time to train the *MotifDisco* causal discovery framework in seconds for (a) different numbers of traces n , (b) motif lengths τ and (c) motif set sizes $|\mathcal{M}|$. Training was for 10 epochs in all experiments. As to be expected, training time increases for larger n and $|\mathcal{M}|$. Interestingly, time reduces as the τ increases, which may in part be because larger τ s mean there are less total motifs (i.e., $|\mathcal{M}|$ is smaller).

Use Cases. We next evaluate the suitability of Motif Causality to help in three downstream tasks: Forecasting, Anomaly Detection and Clustering. For each use case, we build a simple base model and integrate MC following the architecture descriptions in Section 5. We then compute a set of evaluation metrics to compare the performance between the base model and the MC integrated one.

Forecasting. For the forecasting task, we use a simple bidirectional LSTM as our base model. We set the sliding window size, τ and forecasting window to 6 timesteps. We train the causal discovery

Table 1: Use Case Performance Summary. The arrow indicates desired result direction and bold values indicate the best performing model.

Dataset	Model	Forecasting RMSE (\downarrow)	Anomaly Detection				Clustering			
			Accuracy (\uparrow)	F1 (\uparrow)	Sensitivity (\uparrow)	Specificity (\uparrow)	C-Index (\downarrow)	SSE (\downarrow)	Silhouette (\uparrow)	Caliński Harabasz (\uparrow)
Glucose	Base	0.22 \pm 0.05	0.83 \pm 0.02	0.80 \pm 0.03	0.67 \pm 0.02	1.0 \pm 0.0	0.086 \pm 1e-6	477.0 \pm 1e-3	0.318 \pm 1e-2	490.95 \pm 6e-2
	MC	0.18 \pm 0.07	0.92 \pm 0.02	0.92 \pm 0.02	1.0 \pm 0.0	0.85 \pm 0.03	0.085 \pm 3e-5	473.79 \pm 5e-3	0.332 \pm 2e-3	496.24 \pm 5e-4
ECG	Base	0.30 \pm 0.14	0.72 \pm 0.10	0.74 \pm 0.11	0.59 \pm 0.13	0.70 \pm 0.09	0.041 \pm 6e-2	821.10 \pm 2e-3	0.426 \pm 3e-3	970.82 \pm 4e-3
	MC	0.17 \pm 0.12	0.80 \pm 0.11	0.75 \pm 0.09	0.83 \pm 0.09	0.70 \pm 0.12	0.040 \pm 3e-2	820.46 \pm 1e-2	0.428 \pm 4e-3	972.27 \pm 2e-4
Resp	Base	0.32 \pm 0.11	0.65 \pm 0.12	0.73 \pm 0.13	0.31 \pm 0.14	0.91 \pm 0.15	0.075 \pm 2e-3	476.6 \pm 3e-4	0.430 \pm 3e-2	1006.12 \pm 5e-2
	MC	0.26 \pm 0.14	0.71 \pm 0.12	0.74 \pm 0.11	0.65 \pm 0.12	0.86 \pm 0.14	0.073 \pm 5e-3	476.5 \pm 2e-3	0.432 \pm 4e-2	1007.65 \pm 3e-4

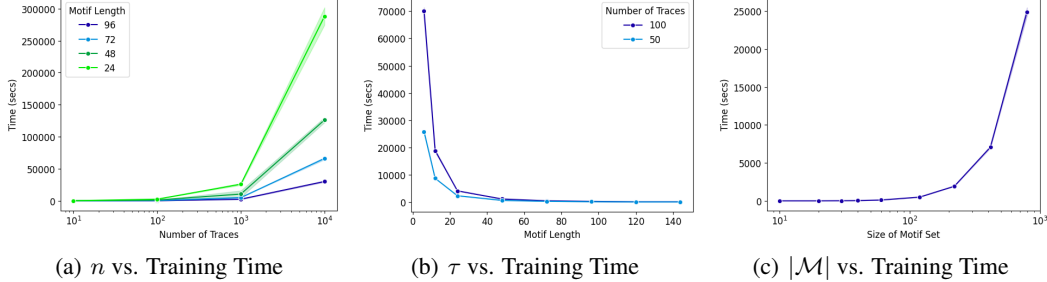


Figure 8: Scalability for glucose traces varying (a) # of traces (n), (b) motif lengths (τ) and (c) motif set sizes ($|\mathcal{M}|$). Results for the other data streams are available in Appx. A.3.2.

and forecasting models for 20 and 2000 epochs, respectively. The Root Mean Square Error (RMSE) is reported in Table 1; the MC model outperforms the base one for all datasets.

Anomaly Detection. For this task, we build a simple autoencoder consisting of stacks of sequential dense layers. In the base model, an anomaly is detected if the Mean Absolute Error (MAE) of the reconstructed data (i.e., the trace fed through the encoder and then returned via the decoder) is less than a reconstruction threshold which we set as the standard deviation of the mean of the normal (non-anomalous) training data. In the MC-integrated version, we detect an anomaly if the predicted MC value between the previous time chunk (motif) and the current one is less than the edge prediction threshold θ . We set the sliding window size and τ to 48, θ to 0.1 and train the causal discovery and anomaly models for 10 and 50 epochs, respectively. We compare the models by computing a set of classification metrics including accuracy, F1, Sensitivity and Specificity using the ground truth labeled anomalies. Results are reported in Table 1. For all metrics except Specificity, the MC-integrated model does better. Interestingly, the base model has better Specificity while the MC model has better Sensitivity - this indicates the MC model is better at identifying the anomalies (the true negatives) and the base is better at identifying the normal traces (the true positives). Example anomaly predictions are shown in Figure 15 in A.3.3.

Clustering. We implement a simple K-Means clustering algorithm. In the base model we compute distances between the cluster centroids and other trace data points using Discrete Time Warping (DTW) [39]. In the MC-integrated version we compute the distances as DTW + MC. We set the number of clusters $k = 3$, and $\tau = 48$. Causal discovery and clustering models were trained for 20 epochs. We compute a set of clustering evaluation metrics including C-Index [42], Sum of Squared Error (SSE) [43], Silhouette score [44], and Caliński Harabasz score [45], reported in Table 1. Across all metrics the MC version does better, indicating adding an element of causality may help clustering.

7 Conclusion & Limitations

In this paper we presented *MotifDisco*, the first causal discovery framework to infer Motif Causality amongst time series motifs. By providing a new method to learn and quantify relationships amongst motifs, *MotifDisco* may facilitate the development of advanced, high performing technologies for event-based time series. As shown by the scalability experiments, for very large \mathcal{M} and n (e.g., $n \geq 10000$) the runtime can take several hours. There are many opportunities in the training framework to further optimize the runtime. For example, MC is currently computed between each edge in a batch sequentially; using sampling or parallelization would significantly speed up the training time. Additionally, a challenge of this work is that there is no known causal structure

available, so it was not possible to evaluate the learned motif causal graphs against some ground truth. However, as evidenced by the use case evaluation, using a relatively simple integration of MC with naive base models resulted in significant performance improvements for all three use cases, providing some evidence about the potential generalizability and applicability of MC for many real world tasks.

References

- [1] Wenjin Niu, Zijun Gao, Liyan Song, and Lingbo Li. Comprehensive review and empirical evaluation of causal discovery algorithms for numerical data. *arXiv preprint arXiv:2407.13054*, 2024.
- [2] Clive WJ Granger. Investigating causal relations by econometric models and cross-spectral methods. *Econometrica: journal of the Econometric Society*, pages 424–438, 1969.
- [3] Thomas Schreiber. Measuring information transfer. *Physical review letters*, 85(2):461, 2000.
- [4] Chang Gong, Di Yao, Chuzhe Zhang, Wenbin Li, and Jingping Bi. Causal discovery from temporal data: An overview and new perspectives. *arXiv preprint arXiv:2303.10112*, 2023.
- [5] Charles K Assaad, Emilie Devijver, and Eric Gaussier. Survey and evaluation of causal discovery methods for time series. *Journal of Artificial Intelligence Research*, 73:767–819, 2022.
- [6] Penghang Liu, Valerio Guarrasi, and Ahmet Erdem Sariyüce. Temporal network motifs: Models, limitations, evaluation. *IEEE Transactions on Knowledge and Data Engineering*, 35(1):945–957, 2021.
- [7] Lauri Kovanen, Márton Karsai, Kimmo Kaski, János Kertész, and Jari Saramäki. Temporal motifs in time-dependent networks. *Journal of Statistical Mechanics: Theory and Experiment*, 2011(11):P11005, 2011.
- [8] Jialin Chen and Rex Ying. Tempme: Towards the explainability of temporal graph neural networks via motif discovery. *Advances in Neural Information Processing Systems*, 36, 2024.
- [9] Xuexin Chen, Ruichu Cai, Yuan Fang, Min Wu, Zijian Li, and Zhifeng Hao. Motif graph neural network. *IEEE Transactions on Neural Networks and Learning Systems*, 2023.
- [10] Ming Jin, Yuan-Fang Li, and Shirui Pan. Neural temporal walks: Motif-aware representation learning on continuous-time dynamic graphs. *Advances in Neural Information Processing Systems*, 35:19874–19886, 2022.
- [11] Naaek Chinpattanakarn and Chainarong Amornbunchornvej. Framework for variable-lag motif following relation inference in time series using matrix profile analysis. *arXiv preprint arXiv:2401.02860*, 2024.
- [12] Josephine Lamp, Mark Derdzinski, Christopher Hannemann, Joost Van der Linden, Lu Feng, Tianhao Wang, and David Evans. Glucosynth: Generating differentially-private synthetic glucose traces. *Advances in Neural Information Processing Systems*, 36, 2024.
- [13] Uzma Hasan, Emam Hossain, and Md Osman Gani. A survey on causal discovery methods for iid and time series data. *arXiv preprint arXiv:2303.15027*, 2023.
- [14] Ali Shojaie and Emily B Fox. Granger causality: A review and recent advances. *Annual Review of Statistics and Its Application*, 9(1):289–319, 2022.
- [15] Yicheng Pan, Yifan Zhang, Xinrui Jiang, Meng Ma, and Ping Wang. Effcause: Discover dynamic causal relationships efficiently from time-series. *ACM Transactions on Knowledge Discovery from Data*, 18(5):1–21, 2024.
- [16] Alex Tank, Ian Covert, Nicholas Foti, Ali Shojaie, and Emily B Fox. Neural granger causality. *IEEE Transactions on Pattern Analysis and Machine Intelligence*, 44(8):4267–4279, 2021.
- [17] Sindy Löwe, David Madras, Richard Zemel, and Max Welling. Amortized causal discovery: Learning to infer causal graphs from time-series data. In *Conference on Causal Learning and Reasoning*, pages 509–525. PMLR, 2022.

- [18] Paolo Bonetti, Alberto Maria Metelli, and Marcello Restelli. Causal feature selection via transfer entropy. In *2024 International Joint Conference on Neural Networks (IJCNN)*, pages 1–10. IEEE, 2024.
- [19] Bahareh Najafi, Saeedeh Parsaeefard, and Alberto Leon-Garcia. Entropy-aware time-varying graph neural networks with generalized temporal hawkes process: Dynamic link prediction in the presence of node addition and deletion. *Machine Learning and Knowledge Extraction*, 5(4): 1359–1381, 2023.
- [20] Abdul Fatir Ansari, Lorenzo Stella, Caner Turkmen, Xiyuan Zhang, Pedro Mercado, Huibin Shen, Oleksandr Shchur, Syama Sundar Rangapuram, Sebastian Pineda Arango, Shubham Kapoor, et al. Chronos: Learning the language of time series. *arXiv preprint arXiv:2403.07815*, 2024.
- [21] Ling Chen, Donghui Chen, Zongjiang Shang, Binqing Wu, Cen Zheng, Bo Wen, and Wei Zhang. Multi-scale adaptive graph neural network for multivariate time series forecasting. *IEEE Transactions on Knowledge and Data Engineering*, 35(10):10748–10761, 2023.
- [22] Falih Gozi Febrinanto, Kristen Moore, Chandra Thapa, Mujie Liu, Vidya Saikrishna, Jiangang Ma, and Feng Xia. Entropy causal graphs for multivariate time series anomaly detection. *arXiv preprint arXiv:2312.09478*, 2023.
- [23] Ziheng Duan, Haoyan Xu, Yida Huang, Jie Feng, and Yueyang Wang. Multivariate time series forecasting with transfer entropy graph. *Tsinghua Science and Technology*, 28(1):141–149, 2022.
- [24] Yuhang Wu, Mengting Gu, Lan Wang, Yusan Lin, Fei Wang, and Hao Yang. Event2graph: Event-driven bipartite graph for multivariate time-series anomaly detection. *arXiv preprint arXiv:2108.06783*, 2021.
- [25] Patrick Schäfer and Ulf Leser. Motiflets: Simple and accurate detection of motifs in time series. *Proceedings of the VLDB Endowment*, 16(4):725–737, 2022.
- [26] Lexiang Ye and Eamonn Keogh. Time series shapelets: a new primitive for data mining. In *ACM SIGKDD International Conference on Knowledge Discovery and Data Mining*, 2009.
- [27] Lionel Barnett, Adam B Barrett, and Anil K Seth. Granger causality and transfer entropy are equivalent for gaussian variables. *Physical review letters*, 103(23):238701, 2009.
- [28] Chainarong Amornbunchornvej, Elena Zheleva, and Tanya Berger-Wolf. Variable-lag granger causality and transfer entropy for time series analysis. *ACM Transactions on Knowledge Discovery from Data (TKDD)*, 15(4):1–30, 2021.
- [29] Nicolás Iribarra, Kevin Michell, Cristhian Bermeo, and Werner Kristjanpoller. A multi-head attention neural network with non-linear correlation approach for time series causal discovery. *Applied Soft Computing*, 165:112062, 2024.
- [30] Karim Assaad, Emilie Devijver, Eric Gaussier, and Ali Ait-Bachir. A mixed noise and constraint-based approach to causal inference in time series. In *Machine Learning and Knowledge Discovery in Databases. Research Track: European Conference, ECML PKDD 2021, Bilbao, Spain, September 13–17, 2021, Proceedings, Part I 21*, pages 453–468. Springer, 2021.
- [31] Jie Sun, Dane Taylor, and Erik M Bollt. Causal network inference by optimal causation entropy. *SIAM Journal on Applied Dynamical Systems*, 14(1):73–106, 2015.
- [32] Claude Elwood Shannon. A mathematical theory of communication. *The Bell system technical journal*, 27(3):379–423, 1948.
- [33] Petr Jizba, Hagen Kleinert, and Mohammad Shefaat. Rényi’s information transfer between financial time series. *Physica A: Statistical Mechanics and its Applications*, 391(10):2971–2989, 2012.
- [34] Petr Jizba, Hynek Lavička, and Zlata Tabachová. Causal inference in time series in terms of rényi transfer entropy. *Entropy*, 24(7):855, 2022.

- [35] Osvaldo A Rosso, Susana Blanco, Juliana Yordanova, Vasil Kolev, Alejandra Figliola, Martin Schürmann, and Erol Başar. Wavelet entropy: a new tool for analysis of short duration brain electrical signals. *Journal of neuroscience methods*, 105(1):65–75, 2001.
- [36] Christoph Bandt and Bernd Pompe. Permutation entropy: a natural complexity measure for time series. *Physical review letters*, 88(17):174102, 2002.
- [37] Will Hamilton, Zhitao Ying, and Jure Leskovec. Inductive representation learning on large graphs. *Advances in neural information processing systems*, 30, 2017.
- [38] Simon Behrendt, Thomas Dimpfl, Franziska J Peter, and David J Zimmermann. Rtransfer-entropy—quantifying information flow between different time series using effective transfer entropy. *SoftwareX*, 10:100265, 2019.
- [39] Hiroaki Sakoe and Seibi Chiba. Dynamic programming algorithm optimization for spoken word recognition. *IEEE transactions on acoustics, speech, and signal processing*, 26(1):43–49, 1978.
- [40] Halis Kaan Akturk, Robert Dowd, Kaushik Shankar, and Mark Derdzinski. Real-world evidence and glycemic improvement using Dexcom G6 features. *Diabetes Technology & Therapeutics*, 23(S1):S–21, 2021.
- [41] SRBR Samsung R&D Institute Brazil, Otávio A. B. Penatti, Carlos Caetano, Vinicius H. Cene, Ivandro Sanches, Victor V. Gomes, Lizeth S. B. Cabrera, Thomas Beltrame, Wonkyu Lee, and Sanghyun Baek. MIMIC-BP. *Harvard Dataverse*, 2023. doi: 10.7910/DVN/DBM1NF. URL <https://doi.org/10.7910/DVN/DBM1NF>.
- [42] Lawrence J Hubert and Joel R Levin. A general statistical framework for assessing categorical clustering in free recall. *Psychological bulletin*, 83(6):1072, 1976.
- [43] J Macqueen. Some methods for classification and analysis of multivariate observations. In *Proceedings of 5-th Berkeley Symposium on Mathematical Statistics and Probability/University of California Press*, 1967.
- [44] Peter J Rousseeuw. Silhouettes: a graphical aid to the interpretation and validation of cluster analysis. *Journal of computational and applied mathematics*, 20:53–65, 1987.
- [45] Tadeusz Caliński and Jerzy Harabasz. A dendrite method for cluster analysis. *Communications in Statistics-theory and Methods*, 3(1):1–27, 1974.

A Technical Appendices and Supplementary Material

A.1 Additional Introduction

Sample Traces. Sample real traces and motifs from glucose are available in Figure 1. Sample traces and motifs for ECG are shown in Figure 9 and for respiration (resp) are shown in Figure 10.

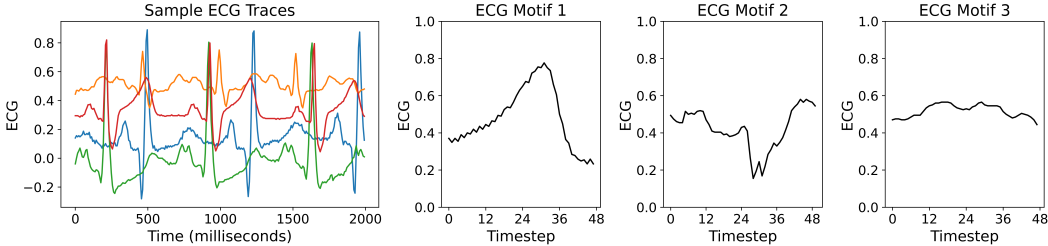


Figure 9: Real ECG Traces and Sample Motifs for $\tau = 48$.

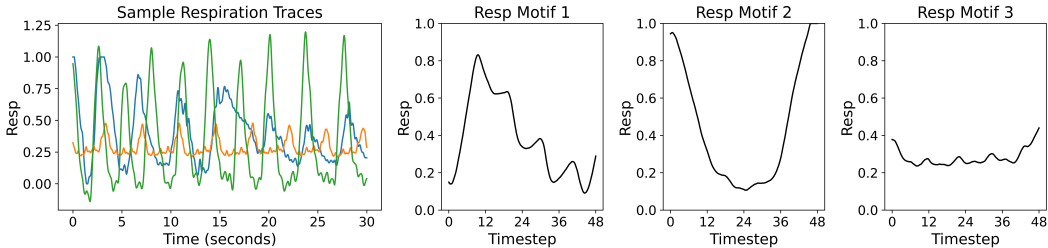


Figure 10: Real Respiration (Resp) Traces and Sample Motifs for $\tau = 48$.

A.2 Additional Methodology

Extracting Motifs. We assume there is a consistent, conclusive way to pull motifs from the traces. Motif discovery is outside the scope of this work; discussion about motif extraction methods and artifacts is outside the scope of the paper since the problem of how to extract motifs has been widely solved (e.g., there are many nice methods to pull out motifs in an intelligent manner, given some criteria, and specific to different disciplines, such as [11, 25, 26]). Our framework is amenable to any motif extraction method, and, as evidenced by our results, works even when using simple or heuristic motif extraction methods, such as chopping.

MC Computation in Link Predictor. To implement the MC computation, we adapt existing Transfer Entropy libraries [38] and compute the conditional entropy function (i.e., $H(\mu)$, Shannon’s or Rényi entropy) using the histogram method. A simplified depiction is shown in Figure 11. Essentially, motif time series values are binned into a histogram. Distributions between motifs can be compared to determine how much uncertainty about future predictions of the motif is reduced in the distribution. For example, in 11(a) when computing MC for μ^i , μ^j covers a larger distribution, resulting in a large reduction in uncertainty and higher motif causality, whereas 11(b) μ^z covers hardly any new distribution compared to the status quo ($H(\mu^i|\mathcal{K})$), resulting in a small reduction in uncertainty and low causality for μ^z .

Clustering Use Case. To integrate Motif Causality with a basic clustering algorithm, we use the motif causality values as an additional distance metric. The intuition is to add an element of *causality* to the clustering, such that as the algorithm learns, MC values within each cluster will be minimized and similar data points within the cluster should be *motif causal* of each other. An example is shown in Figure 12: the MC value between the blue centroid and the blue data point to the right is high with 0.9, whereas the MC between the blue centroid and the green data point belonging to a different cluster is low at 0.11.

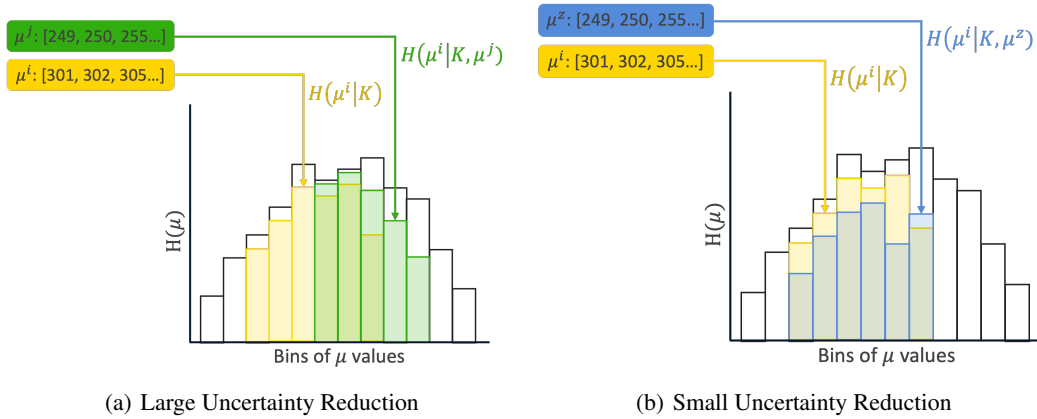


Figure 11: Depiction of Conditional Entropy $H(\mu)$ computation using the histogram method: when computing MC for μ^i , (a) μ^j results in a large uncertainty reduction; (b) μ^z has a small reduction.

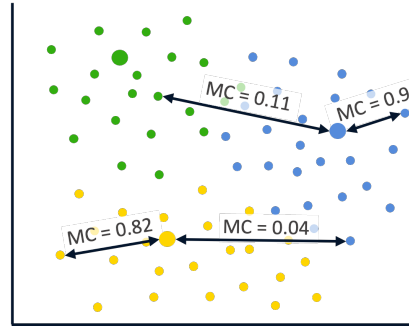


Figure 12: Depiction of Clustering Model integrated with MC.

A.3 Additional Evaluation

As mentioned in Section 2, there is no prior work on quantifying causality amongst motifs, and we cannot compare with existing Granger causal techniques because their framework set-up or model assumptions do not hold. Specifically, they have one or more of the following issues:

- Compose relations between only two time series, and cannot find relationships amongst a *set* of motifs or traces [4, 28].
- Formulate causality based on various statistical properties amongst *variables*, such as variable-based correlation and density-, classification- and prediction-based error measures computed between multivariate features [18, 28, 29]. These assumptions do not hold for *univariate* time series motifs.
- Compose causal relationships over time series using repeated statistical measures or temporal dynamics, e.g., things like learning implicit repeated patterns, or computing sufficiency or faithfulness hypotheses over lags across the full time series [12, 15, 16, 17, 19, 30, 31]. These methods do not work for motifs because they are short time series (so there would be no repeated patterns, nor will statistical hypotheses like sufficiency or faithfulness hold since they are not evaluating multiple time lags repeated over a trace).
- Require labels or a known underlying causal structure to guide model training [4, 18, 19], which is not available for our data and many similar event-based data streams.

Therefore, for our evaluation in Section 6, we evaluate our causal discovery framework in terms of scalability and performance for 3 downstream use cases: forecasting, anomaly detection and clustering.

A.3.1 Dataset Details

An overview of characteristics for each dataset is shown in Table 2. The glucose traces are sets of single-day glucose traces randomly sampled across each month from January to December 2022, collected from Dexcom’s G6 Continuous Glucose Monitors (CGMs) [40]. Data was recorded every 5 minutes, resulting in a total of 288 timepoints per trace. Each trace was aligned temporally from 00:00 to 23:59. The ECG and Respiration (resp) traces come from MIMIC-BP [41], a curated dataset collecting common biomedical signals. We use data from a single segment. There are a total of 1523 patients, with data collected for a total of 3750 timepoints, sampled at frequencies of 1 millisecond for ECG and 1 second for Resp.

Table 2: Dataset Characteristics.

Dataset	# Patients	Total # Timepoints	Sampling Frequency
Glucose [40]	300000	288	5 minutes
ECG [41]	1523	3750	1 millisecond
Resp [41]	1523	3750	1 second

A.3.2 Additional Scalability Results

Due to space constraints, we report the results for the MIMIC-BP dataset streams of ECG and Respiration (Resp) in Figure 13 and Figure 14 respectively here. As found with the glucose traces, training time increases for larger n and $|\mathcal{M}|$. Time also reduces as the τ increases, which may in part be because larger τ s mean there are less total motifs (i.e., $|\mathcal{M}|$ is smaller). Overall, training time for the Resp dataset takes the longest, perhaps because the Resp traces are the more variable, resulting in more variable (i.e., more noisy) motifs.

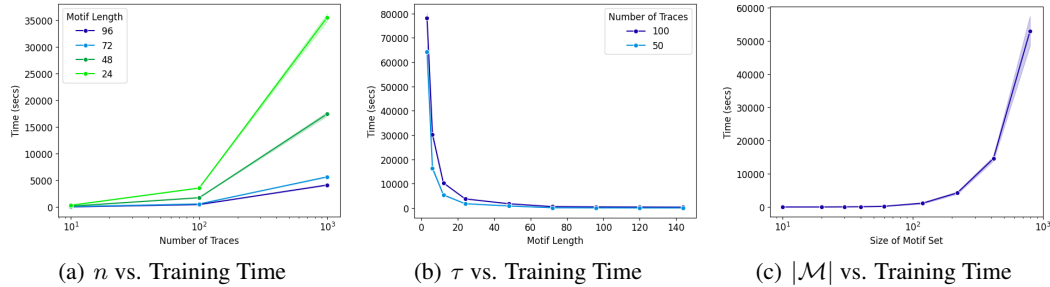


Figure 13: Scalability for ECG traces varying (a) # of traces (n), (b) motif lengths (τ) and (c) motif set sizes ($|\mathcal{M}|$).

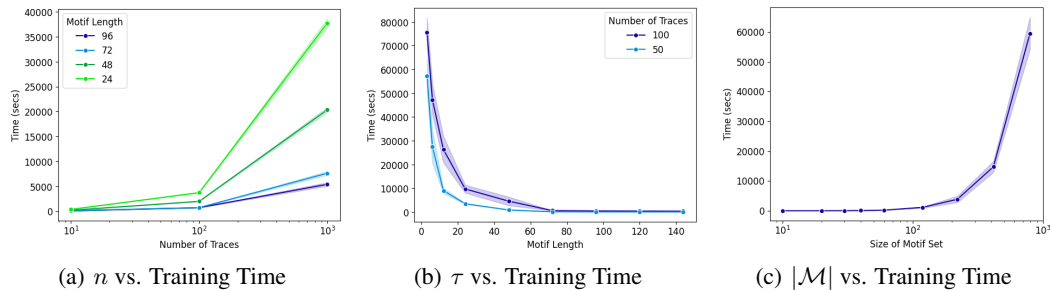


Figure 14: Scalability for respiration traces varying (a) # of traces (n), (b) motif lengths (τ) and (c) motif set sizes ($|\mathcal{M}|$).

A.3.3 Additional Use Case Results

Anomaly Detection. Example anomaly predictions are shown in Figure 15. Each graph plots the original input trace (in blue) and the reconstructed trace (in red, trace fed through the encoder + decoder) with the error between the two shaded in red. The window segments (dashed black lines) correspond to the motif and prediction window size and the model predictions are annotated in each window, colored by the correctness of the prediction. Green indicates a correct prediction, red indicates an incorrect one.

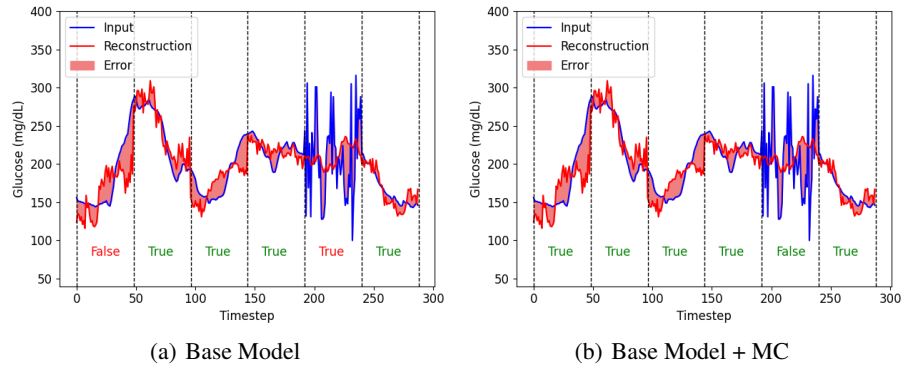


Figure 15: Anomaly Detection for a trace with an obvious anomaly using the (a) base model and the model integrated with MC (b). False means an anomaly was predicted and the color corresponds to correctness of the prediction: green is a correct prediction, red is an incorrect one.

A.3.4 Example Motif Causality Between Motifs

Learned motif causality values between sample motifs for glucose are illustrated in Figure 16 and Figure 17.

A.4 Additional Conclusion

Broader Impacts & Safeguards. The core contribution of this project is the development of *MotifDisco*, the first causal discovery framework to infer Motif Causality amongst time series motifs. In terms of broader impacts, *MotifDisco* may facilitate the development of advanced, high performing technologies for event-based time series by providing a new method to learn and quantify relationships amongst motifs. Since this project presents a foundational research framework that can be applied in many diverse settings and scenarios, discussion of deployments is outside the scope of this work. However, the authors note that any deployment using this framework may need to integrate the necessary measures and safeguards to reduce the risk of possible societal harms (particularly for applications in medical settings), such as data release and consent frameworks, and strict privacy and security measures.

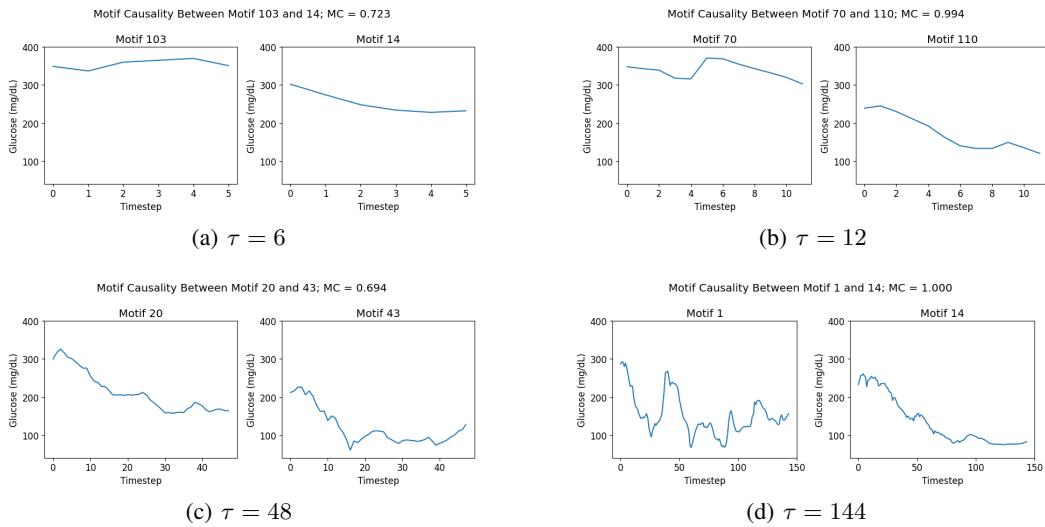


Figure 16: Example High Motif Causality values between different motif sizes for Glucose.

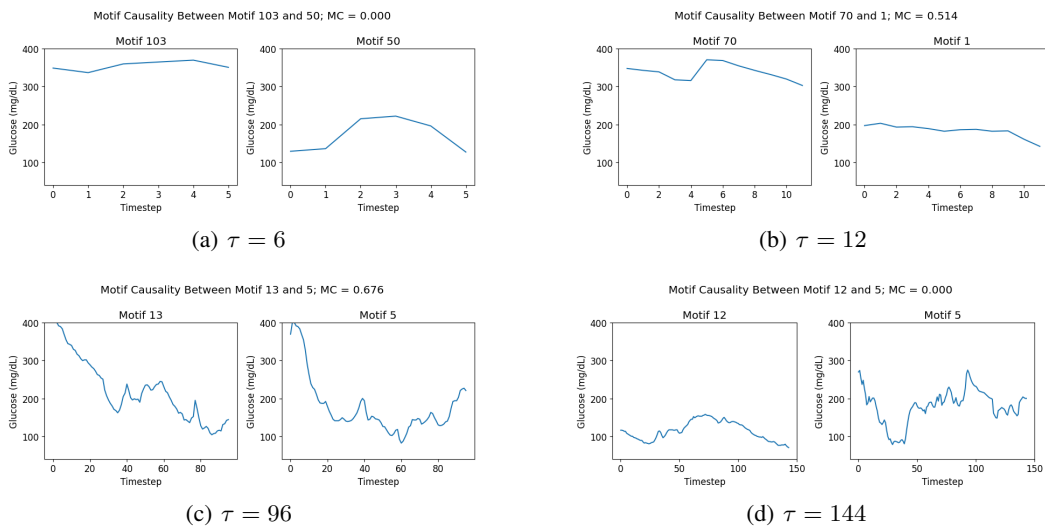


Figure 17: Example Low Motif Causality values between different motif sizes for Glucose.